

Synthesis and characterisation of $\text{LiNi}_{1-x-y}\text{Co}_x\text{Al}_y\text{O}_2$ cathodes for lithium-ion batteries by the PVA precursor method

P.H. Duvigneaud*, T. Segato

Chimie Industrielle, CP 165/63, Université Libre de Bruxelles, 50 Av. Fr. D. Roosevelt, 1050 Bruxelles, Belgium

Abstract

Polycrystalline powders of $\text{LiNi}_{1-x}\text{Co}_x\text{O}_2$ and $\text{LiNi}_{1-x-y}\text{Co}_x\text{Al}_y\text{O}_2$ were synthesized at 720 °C from the nitrate-PVA precursor method. The water was removed by two different processes: (i) evaporation-drying at 110 °C, (ii) spray-drying at 150 °C. In both cases a gel is obtained wherein LiNO_3 crystallizes in evaporated-dried samples but not in spray-dried samples which are more amorphous. All precursors give single phase powders with micronic well-shaped grains. The best electrochemical performances are obtained from evaporated samples with a capacity remaining higher than 160 mAh/g for $\text{LiNi}_{0.82}\text{Co}_{0.18}\text{O}_2$ and 140 mAh/g for $\text{LiNi}_{0.82}\text{Co}_{0.13}\text{Al}_{0.05}\text{O}_2$ after 20 cycles. The lower performances of the spray-dried samples seem to be related to Li_2CO_3 formation with subsequent non-stoichiometry as a consequence of the improved homogeneous distribution of the constituent cations in the polymer.

© 2003 Elsevier Ltd. All rights reserved.

Keywords: Batteries; LiNiO_2 ; Electrical properties; Precursors-organic

1. Introduction

LiNiO_2 and LiCoO_2 have attracted interest as cathode materials for 4V rechargeable lithium batteries. Both systems have a layered rock salt structure with the rhomboedral $R3m$ space group. Stoichiometric LiCoO_2 , which is synthesized relatively easily, is widely used in commercial cells. LiNiO_2 is also under consideration due to its lower cost and higher specific capacity. However, high capacity fading on charge–discharge cycling and low thermal stability in the charged state have inhibited its commercialisation so far. These drawbacks are related to the difficulty to obtain stoichiometric LiNiO_2 because high temperature treatments lead to $\text{Li}_{1-x}\text{Ni}_{1+x}\text{O}_2$ which has a partially disordered cationic distribution at the Li site.

Partial substitution for nickel by a transition (Co, Mn)^{1–4} or a non-transition metal (Al, Mg)^{5–7} is expected to improve the two dimensional layered structure and the capacity fading upon cycling. In this study we have investigated $\text{LiNi}_{1-x}\text{Co}_x\text{O}_2$ and $\text{LiNi}_{1-x-y}\text{Co}_x\text{Al}_y\text{O}_2$ compositions which are able to form complete solid solutions in the rhombohedral system.

$\text{LiNi}_{1-x}\text{Co}_x\text{O}_2$ has usually been prepared by the conventional solid state reaction from oxide, carbonate, hydroxide or nitrates mixtures. Synthesis of $\text{LiNi}_{1-x}\text{Co}_x\text{O}_2$ from oxides or carbonates involves heat treatment at ≥ 800 °C. On the other hand, synthesis from pure nitrates is difficult to control. In both cases, lithium deficiency and cation disorder may occur. As an effort to favour the chemical reactions at low temperature (< 750 °C), we have used a polyvinyl alcohol (PVA) as a polymeric carrier in a mixed cation nitrate solution. This technique, which involves the formation of complexes between the cations and the hydroxyl side groups of PVA, thereby limiting the fractional precipitation of metal salts, has recently been processed in the synthesis of various materials such as cements, perovskites and α NaFeO_2 -type phases.^{8,9}

2. Experimental

Samples of target compositions $\text{LiNi}_{0.82}\text{Co}_{0.18}\text{O}_2$ and $\text{LiNi}_{0.82}\text{Co}_{0.13}\text{Al}_{0.05}\text{O}_2$ with excess amounts of lithium between 0 and 4% were synthesized. LiNO_3 , $\text{Ni}(\text{NO}_3)_2 \cdot 6\text{H}_2\text{O}$, $\text{Co}(\text{NO}_3)_2 \cdot 7\text{H}_2\text{O}$ (Fluka p.a.) and $\text{Al}(\text{NO}_3)_3 \cdot 9\text{H}_2\text{O}$ (Merck p.a.) were dissolved in distilled water. Polyvinyl alcohol (PVA, Fluka, $M = 22,000$) was

* Corresponding author.

dissolved in a separate container. The two aqueous solutions were mixed into a dark transparent solution. The ratio between the positively charged valences from the cations and the $-OH$ groups of PVA was ≈ 4 . The water was removed by two different processes: (i) evaporation at $\approx 80^\circ\text{C}$ until a gel formation, followed by a drying treatment in air at 110°C , (ii) spray-drying using a Buchi 190 mini spray-dryer at $\approx 150^\circ\text{C}$. Thermal treatments were performed at 720 and 750°C for 24 h in an oxygen gas flow. The heating rate was $2^\circ\text{C}/\text{min}$.

The X-ray diffraction (XRD) patterns of the powders were recorded using a Siemens D5000 powder diffractometer. The lattice parameters of the nickelates were refined by Rietveld analysis using the Topas P program. Scanning electron microscope (SEM) micrographs were taken with a Jeol JSM 6100 to study the particle morphology. Surface area of the powder was measured by the BET method by using a flow sorb II 2300 from Micromeritics. The Li content of the nickelate powders was determined by atomic absorption (Perkin–Elmer 460). The $(\text{Ni} + \text{Co})^{3+}$ content was analysed by a chemical redox titration using Fe^{++} as a reductor and KMnO_4 as a titrant. Total carbon was analysed with a LECO EC 12.

Thermal evolution was studied by thermo-gravimetric analysis (TGA) on a Setaram MTB 10-8 model and by differential calorimetric analysis (DSC) supplied by Mettler-Toledo, model 821.

Electrochemical properties of the powders were studied by obtaining charge–discharge cycle curves from a coin-type cell of the lithium ion battery between 3.0 and 4.1 V vs metallic Li, using a multichannel battery analyser system from Arbin Co. The powder was mixed with PVDF binder and C. The electrolyte was LiPF_6 dissolved in EC/DMC (1:1).

3. Results and discussion

The precursors obtained from evaporation and drying at 110°C (PE) and from spray-drying at 150°C (PS) have been characterized by XRD.

The precursors of PE-type are partially crystallized into LiNO_3 and a nickel nitrate hydroxyde hydrate $\text{Ni}(\text{NO}_3)_2 \cdot \text{Ni}(\text{OH})_2 \cdot 2\text{H}_2\text{O}$ in which the cobalt and the aluminium are probably associated (Fig. 1, PE110). Conversely, in PS-type precursors, LiNO_3 crystallization is strongly reduced while another Ni salt, i.e. $\text{Ni}(\text{NO}_3)_2 \cdot 2\text{Ni}(\text{OH})_2$ is evidenced (Fig. 1, PS150). In the absence of PVA, crystallisation of pure nitrates $\text{Ni}(\text{NO}_3)_2 \cdot 4\text{H}_2\text{O}$ and $\text{Co}(\text{NO}_3)_2 \cdot 4\text{H}_2\text{O}$ was observed. This means that a PVA-nitrate interaction occurs by which $-\text{NO}_3$ groups are replaced by $-\text{OH}$ groups in the precursor with NO_x evolution. This interaction thus favours the chain-stripping elimination of $-\text{OH}$ and H_2O from PVA, which is known to produce vinyl bonds, chain scission and cyclization reactions at higher temperature. By this process, a better distribution of the cations in the polymer is obtained, specially in PS samples which are more amorphous than PE samples.

The TGA and DSC curves of the PE and PS precursors are given in Figs. 2 and 3.

In all PE samples, total weight losses of $79\% \pm 1\%$ are obtained at 560°C .

In all PS samples, lower weight losses ($62 \pm 1\%$) are found at this temperature. However, additional weight losses of 2% are still recorded up to 800°C (Fig. 2).

Theoretical weight losses of respectively 72.5 , 62.1 and 54.2% are found if we assume that the M^{3+} salt in the precursor is $\text{Ni}(\text{NO}_3)_2 \cdot 4\text{H}_2\text{O}$, $\text{Ni}(\text{NO}_3)_2 \cdot \text{Ni}(\text{OH})_2 \cdot 2\text{H}_2\text{O}$ or $\text{Ni}(\text{NO}_3)_2 \cdot 2\text{Ni}(\text{OH})_2$. The experimental weight losses of PE and PS samples are higher

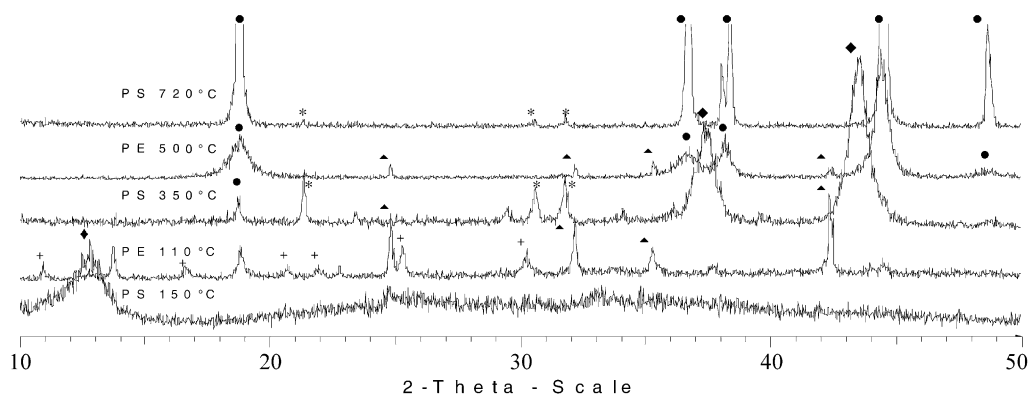


Fig. 1. XRD patterns of $\text{LiNi}_{0.82}\text{Co}_{0.18}\text{O}_2$ precursors synthesized by evaporation-drying at 110°C (PE) and by spray-drying at 150°C (PS) and heated at different temperatures. The designation of symbol is as follows: $\text{Ni}(\text{NO}_3)_2 \cdot \text{Ni}(\text{OH})_2 \cdot 2\text{H}_2\text{O}$ (+), $\text{Ni}(\text{NO}_3)_2 \cdot 2\text{Ni}(\text{OH})_2$ (◆), LiNO_3 (σ), Li_2CO_3 (*), LiNiO_2 (●), $\text{Ni}_{1-x}\text{Li}_x\text{O}$ (▲).

than those predicted from XRD patterns owing to higher water content evidenced by TGA at $<140\text{ }^{\circ}\text{C}$ (Fig. 2).

The main weight losses occur between 140 and $340\text{ }^{\circ}\text{C}$ in PE and PS samples but in different ways. In PE samples, M^{3+} nitrate decomposition ($140\text{--}220\text{ }^{\circ}\text{C}$) and PVA combustion ($240\text{--}320\text{ }^{\circ}\text{C}$) are separated whereas these two phenomena are less distinct in the more homogeneous PS samples ($180\text{--}340\text{ }^{\circ}\text{C}$). The endothermic peak evidenced by DSC at $250\text{ }^{\circ}\text{C}$ (Fig. 3) is ascribed to LiNO_3 melting; it is much steeper in PE sample.

The main exothermic peak in PE ($260\text{ }^{\circ}\text{C}$) and in PS ($280\text{ }^{\circ}\text{C}$) is attributed to PVA combustion, in agreement with TGA. A second exothermic peak, well separated in PE and overlapping the first peak in PS is related to the formation of new phases following the nitrate-PVA decomposition.

The nature of those phases and their evolution has been determined by XRD on samples heated beyond $320\text{ }^{\circ}\text{C}$.

At $350\text{ }^{\circ}\text{C}$, the main XRD peaks are those of the NiO rock-salt structure. Their broadening and shift towards

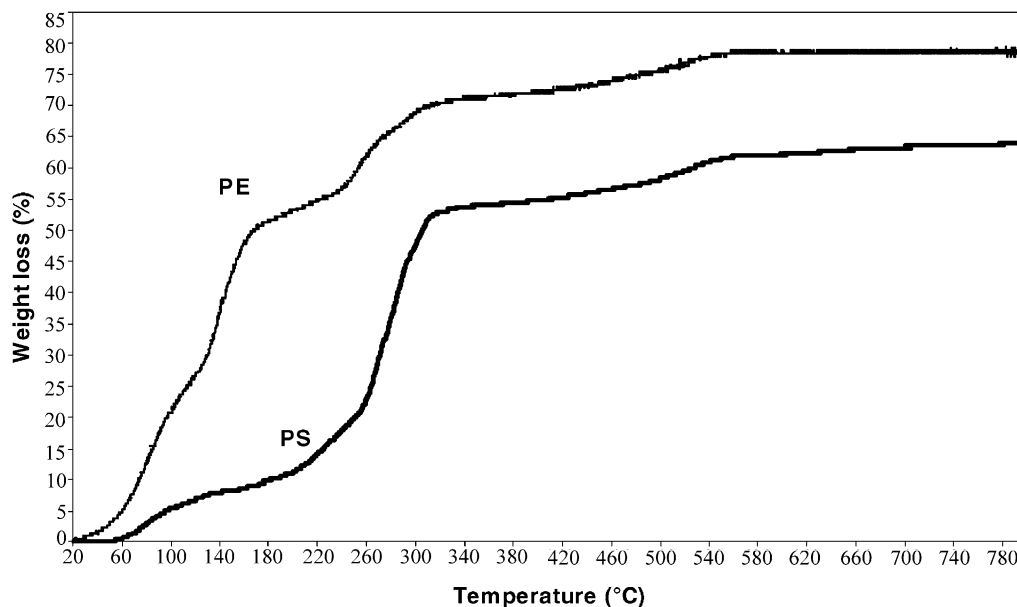


Fig. 2. TG of PE and PS $\text{LiNi}_{0.82}\text{Co}_{0.18}\text{O}_2$ precursors.

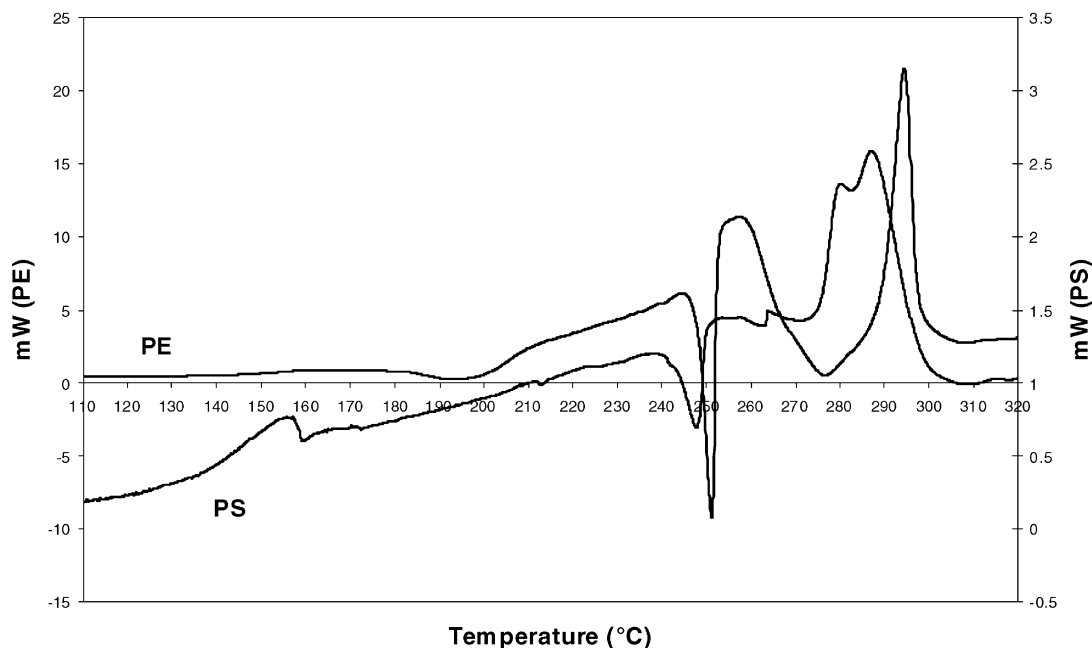


Fig. 3. DSC of PE and PS $\text{LiNi}_{0.82}\text{Co}_{0.18}\text{O}_2$ precursors.

higher 2θ values indicate that part of the lithium enters in NiO to form a composition close to $\text{Ni}_{0.6}\text{Li}_{0.4}\text{O}$ according to JCPDS files. In addition, Li_2CO_3 peaks are present in PS samples as shown in Fig. 1, PS350.

At 500 °C, the XRD peaks of NiO give rise to broadened peaks of rhombohedral LiNiO_2 . In addition, LiNO_3 peaks are still present in PE samples as shown in Fig. 1, PE500.

Thus, the residual weight losses between 320 and 560 °C ($\approx 8\%$) have different origins in PE and PS samples: PE samples lose mainly NO_x from LiNO_3 while PS samples lose mainly CO_2 from Li_2CO_3 . Li_2CO_3 formation in PS samples following the PVA combustion is to be related to the improved dispersion of Li (or very fine LiNO_3 crystals) in the PVA matrix. The better stability of Li_2CO_3 vs LiNO_3 may also explain the weight losses observed beyond 550 °C in PS samples only. Although the XRD patterns shows that well crystallized single phase $\text{LiNi}_{1-x}\text{Co}_x\text{O}_2$ and $\text{LiNi}_{1-x-y}\text{Co}_x\text{Al}_y\text{O}_2$ powders are easily obtained at 720 °C, the presence of Li_2CO_3 traces (Fig. 1, PS720) confirms that complete CO_2 elimination requires higher temperatures.

PE and PS samples heated at 720 °C for 24 h were compared in test coin cells. The discharge capacity for undoped and Al-doped PE and PS compositions as a function of the number of cycles is presented in Figs. 4 and 5.

The PE samples give the highest discharge capacities, i.e. ≈ 160 mAh/g for undoped samples and ≈ 140 mAh/g for Al-doped samples, with a low capacity fading during the first 20 cycles (Fig. 4).

In contrast, all PS samples have lower discharge capacities which only reach 105 mAh/g in the undoped sample with excess Li of 4% (Fig. 5). In Al-doped PS samples, a decrease in capacity of 20 mAh/g with a

lower fading confirms the effect of Al observed in PE samples.

In order to understand why the finer and most homogeneous powders synthesized by spray-drying give lower electrochemical performances than those synthesized by evaporation, further properties of PE and PS powders heated at 720 °C were analysed.

The stoichiometry of lithium was analysed to be ≈ 1 in all PE samples with nominal stoichiometry of 1.03. In PS samples, a more systematic approach gave respectively 0.95, 0.98 and 0.99 in undoped samples and 0.96, 0.98 and 1 in Al-doped samples for nominal stoichiometries of 1, 1.02 and 1.04. Apparently, proper stoichiometries are obtained with Li excesses of ≥ 0.03 .

The oxidized $(\text{Ni} + \text{Co})^{3+}$ content was also analysed. The mean relative values in PE samples are > 0.98 whereas they reach only 0.91 ± 0.01 in PS samples, independently of their lithium concentration. Oxidation is thus less complete in PS samples than in PE samples.

Total carbon in PE samples was analysed to be between 0.4 and 0.5 wt.%. In PS samples, the C contents are 0.61, 0.65 and 0.71% in undoped samples and 0.7, 0.8 and 0.84% in Al-doped samples for nominal stoichiometries of 1, 1.02 and 1.04. This relationship indicates that some carbonation occurs in proportion of the lithium content.

The hexagonal lattice parameters a and c of most PE and PS samples were calculated. The a values are relatively constant whatever the Al and Li content of the samples. Mean values are $a = 2.864 \text{ \AA} \pm 0.001 \text{ \AA}$ for PE samples and $a = 2.868 \text{ \AA} \pm 0.001 \text{ \AA}$ for PS samples. The mean c values in Al-undoped samples are significantly higher in PS ($14.176 \text{ \AA} \pm 0.002 \text{ \AA}$) than in PE ($14.164 \text{ \AA} \pm 0.002 \text{ \AA}$). Moreover the c parameters increase

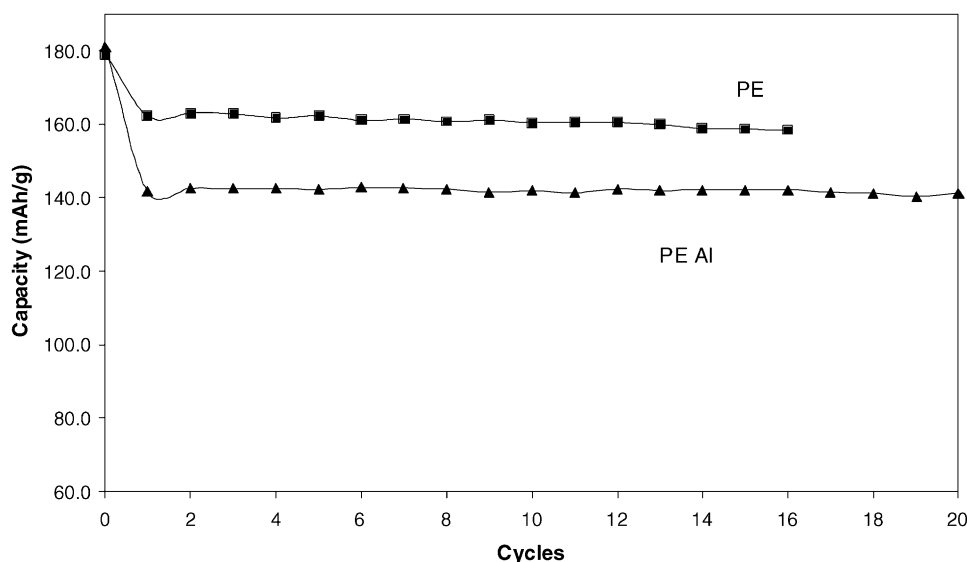


Fig. 4. Discharge capacity (mAh/g) of a coin cell with a cathode made from $\text{LiNi}_{0.82}\text{Co}_{0.18}\text{O}_2$ (PE) and $\text{LiNi}_{0.82}\text{Co}_{0.13}\text{Al}_{0.05}\text{O}_2$ (PE Al) samples at the C/10 rate.

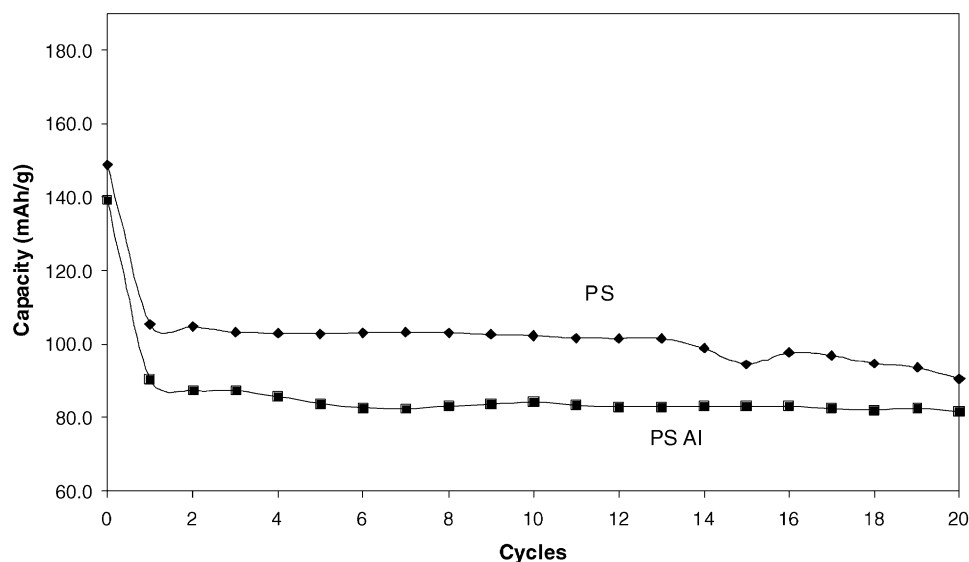


Fig. 5. Discharge capacity (mAh/g) of a coin cell with a cathode made from $\text{LiNi}_{0.82}\text{Co}_{0.18}\text{O}_2$ (PS) and $\text{LiNi}_{0.82}\text{Co}_{0.13}\text{Al}_{0.05}\text{O}_2$ (PS Al) samples at the C/10 rate.

in Al-doped samples ($14.190\text{\AA} \pm 0.002\text{\AA}$ in PS and $14.177\text{\AA} \pm 0.002\text{\AA}$ in PE). This result, which is inconsistent with the smaller ionic radius of Al^{3+} in Ni^{3+} 3b sites was previously reported^{5,6} but not interpreted.

The c/a ratio as well as the intensity ratio of (104) and (003) peaks is considered a measure of cation mixing on Li 3a sites. Our values of PE and PS undoped (4.94) and Al-doped samples (4.95) seem in agreement with the expected 2D-layer structure since lattices with large cation mixing have lower c/a ratios, i.e. 4.89–4.91.^{2,5} Nevertheless, the higher c values in PS samples and the difference in Ni occupancy at 3a Li planes (0.4% in PE, 1.5–2% in PS) evidenced by Rietveld analysis are consistent with a significant non-stoichiometry¹⁰ such as $\text{Li}_{1-x}\text{Ni}_x^{2+}\text{Ni}_{1-x-y}^{3+}\text{Ni}_y^{2+}\text{Co}_{3y}^{3+}\text{O}_2$ in PS compositions which is confirmed by the oxidized $(\text{Ni} + \text{Co})^{3+}$ measurements.

The apparent proper Li stoichiometries obtained with Li excesses ≥ 0.03 are probably less than 1 in PS samples since part of total lithium analysed is carbonated.

The above results are thus coherent to explain the differences in electrochemical properties of PE and PS samples. Carbonation of PS samples is favoured by (i) the better Li dispersion in the polymer matrix preventing LiNO_3 crystallisation, (ii) the higher powder specific surface ($1.5\text{ m}^2/\text{g}$ instead of $0.5\text{ m}^2/\text{g}$ in PE) exposed at 720°C .¹¹ Carbonate formation leads to non-stoichiometry with Ni^{3+} reduction and concomitant degradation of Li (de)intercalation in the lattice.

4. Conclusions

The nitrate-PVA precursor method is a soft-solution process which is able to give in a single heating step up

to 720°C a powder having a discharge capacity remaining higher than 160 mAh/g for $\text{LiNi}_{0.8}\text{Co}_{0.2}\text{O}_2$ and 140 mAh/g for a similar sample doped with 5% Al. However, such performances can be strongly reduced by Li_2CO_3 formation following the PVA combustion step at $\approx 300^\circ\text{C}$, leading to non-stoichiometry. The origin of Li_2CO_3 formation is to be related to the drying conditions of the precursor. High temperature spray-drying (150°C) results in increasing the constituent cations dispersion in the polymer framework which favours Li_2CO_3 formation. In contrast, evaporation and drying at 110°C favours LiNO_3 and $(\text{Ni}, \text{Co}, \text{Al})$ nitrate hydroxide hydrate crystallization apart from the polymer in the precursor, preventing Li_2CO_3 formation.

Acknowledgements

The authors are grateful to Dr O. Van Volden and Dr L. Canet for experiments and useful discussions; to Erachem–Comilog S.A. for electrochemical measurements. Financial support has been provided by the Region Wallonne (First-Europe 99/46539).

References

1. Zhecheva, E. and Stoyanova, R., Stabilisation of the layered crystal structure of LiNiO_2 by Co substitution. *Solid State Ionics*, 1993, **66**, 143–149.
2. Rougier, A., Saadoune, I., Gravereau, P., Willmann, P. and Delmas, C., Effect of cobalt substitution on cationic distribution in $\text{LiNi}_{1-y}\text{Co}_y\text{O}_2$ electrode materials. *Solid State Ionics*, 1996, **90**, 83–90.
3. Glover, R. K. B., Yonemura, M., Hirano, A., Kanno, R., Kawamoto, Y., Murphy, C., Mitchell, B. J. and Richardson,

- J. W., The control of non-stoichiometry in lithium nickel-cobalt oxides. *J. Power Sources*, 1999, **81–82**, 535–541.
4. Cho, J., Kim, G. and Lim, H. S., Effect of preparation methods of cathode materials of $\text{LiNi}_{1-x}\text{Co}_x\text{O}_2$ on their chemical structure and electrode performance. *J. Electrochem. Soc.*, 1999, **146**(10), 3571–3576.
 5. Madhavi, S., Subba Rao, G. V., Chowdari, B. V. R. and Li, S. F. Y., Effect of aluminium doping on cathodic behaviour of $\text{LiNi}_{0.7}\text{Co}_{0.3}\text{O}_2$. *J. Power Sources*, 2001, **93**, 156–162.
 6. Ohzuku, T., Ueda, A. and Kouguchi, M., Synthesis and characterisation of $\text{LiAl}_{1/4}\text{Ni}_{3/4}\text{O}_2$ for lithium-ion batteries. *J. Electrochem. Soc.*, 1995, **142**(12), 4033–4039.
 7. Pouillier, C., Pertion, F., Biensan, Ph., Pérès, J. P., Broussely, M. and Delmas, C., Effect of magnesium substitution on the cycling behavior of lithium nickel cobalt oxide. *J. Power Sources*, 2000, **96**, 293–302.
 8. Kweon, H.-J., Kim, G. B., Lim, H. S., Nam, S. S. and Park, D. G., Synthesis of $\text{LiNi}_{0.85}\text{Co}_{0.15}\text{O}_2$ by the PVA-precursor method and charge-discharge characteristics of a lithium ion battery using this material as cathode. *J. Power Sources*, 1999, **83**, 84–92.
 9. Lee, S. J., Benson, E. A. and Kriven, W. M., Preparation of Portland cement components by poly(vinyl alcohol) solution polymerisation. *J. Am. Ceram. Soc.*, 1999, **82**(8), 2049–2055.
 10. Hirano, A., Kanno, R., Kawamoto, Y., Takeda, Y., Yamaura, K., Takano, M., Ohyama, K., Ohashi, M. and Yamaguchi, Y., Relationships between non-stoichiometry and physical properties in LiNiO_2 . *Solid State Ionics*, 1995, **78**, 123–131.
 11. Matsumoto, K., Kuzuo, R., Takeya, K. and Yamanaka, A., Effects of CO_2 in air on Li deintercalation from $\text{LiNi}_{1-x-y}\text{Co}_x\text{Al}_y\text{O}_2$. *J. Power Sources*, 1999, **81–82**, 558–561.